

Spatial coherence control of xuv supercontinuum generation by two-color laser field

Shaoyi Wang,¹ Weiyi Hong,^{1,2} Qingbin Zhang,¹ Kunlong Liu,¹
Xiaosong Zhu,¹ Peixiang Lu^{1,3,*}

¹Wuhan National Laboratory for Optoelectronics, Huazhong University of Science and Technology, Wuhan 430074, China

²hongweiyi@mail.hust.edu.cn

³State Key Laboratory of Precision Spectroscopy, East China Normal University, Shanghai 200062, China

*lupeixiang@mail.hust.edu.cn

Abstract: We investigate the spatial characteristics of xuv supercontinuum generation in the two-color laser field consisting of a fundamental and a weak second harmonic field. By optimizing the synthesized two-color field, the spatial profile of the xuv supercontinuum varies from annular-like to Gaussian-like and then the spatial quality is improved effectively, which is beneficial for its potential applications. Moreover, our calculation shows that the spatial quality of the supercontinuum is stable when the intensity of the controlling field varies in the acceptable fluctuation.

© 2011 Optical Society of America

OCIS codes: (190.2620) Frequency conversion; (190.4160) Multiharmonic generation; (320.0320) Ultrafast optics.

References and links

1. R. Kienberger, E. Goulielmakis, M. Uiberacker, A. Baltuska, V. Yakovlev, F. Bammer, A. Scrinzi, Th. Westerwalbesloh, U. Kleineberg, U. Heinzmann, M. Drescher, and F. Krausz, "Atomic transient recorder," *Nature* **427**, 817-821 (2004).
2. A. E. Kaplan, "Subfemtosecond Pulses in Mode-Locked 2π Solitons of the Cascade Stimulated Raman Scattering," *Phys. Rev. Lett.* **73**, 1243 (1994).
3. K. Lee, Y. H. Cha, M. S. Shin, B. H. Kim, and D. Kim, "Relativistic nonlinear Thomson scattering as attosecond x-ray source," *Phys. Rev. E* **67**, 026502 (2003).
4. P. Lan, P. Lu, W. Cao, and X. Wang, "Attosecond and zeptosecond x-ray pulses via nonlinear Thomson backscattering," *Phys. Rev. E* **72**, 066501 (2005).
5. M. Hentschel, R. Kienberger, Ch. Spielmann, G. A. Reider, N. Milosevic, T. Brabec, P. Corkum, U. Heinzmann, M. Drescher, and F. Krausz, "Attosecond metrology," *Nature* **414**, 509-513 (2001).
6. T. Pfeifer, L. Gallmann, M. J. Abel, P. M. Nagel, D. M. Neumark, and S. R. Leone, "Heterodyne Mixing of Laser Fields for Temporal Gating of High-order Harmonic Generation," *Phys. Rev. Lett.* **97**, 163901 (2006).
7. I. P. Christov, M. M. Murnane, and H. C. Kapteyn, "High-harmonic generation of Attosecond Pulse in the 'Single-Cycle' Regime," *Phys. Rev. Lett.* **78**, 1251 (1997).
8. P. Lan, P. Lu, W. Cao, and X. Wang, "Efficient generation of an isolated single-cycle attosecond pulse," *Phys. Rev. A* **76**, 043808 (2007).
9. W. Cao, P. Lu, P. Lan, X. Wang, and G. Yang, "Efficient isolated attosecond pulse generation with a multi-cycle two-color laser field," *Opt. Express* **15**, 530 (2007).
10. E. Goulielmakis, M. Schultze, M. Hofstetter, V. S. Yakovlev, J. Gagnon, M. Uiberacker, A. L. Aquila, E. M. Gullikson, D. T. Attwood, R. Kienberger, F. Krausz, and U. Kleineberg, "Single-Cycle Nonlinear Optics," *Science* **320**, 1614-1617 (2008).
11. P. B. Corkum, "Plasma Perspective on Strong-Field Multiphoton Ionization," *Phys. Rev. Lett.* **71**, 1994 (1993).

12. Z. H. Chang, "Single attosecond pulse and xuv supercontinuum in the high-order harmonic plateau," *Phys. Rev. A* **70**, 043802 (2004).
13. Q. Zhang, P. Lu, P. Lan, W. Hong, and Z. Yang, "Multi-cycle laserdriven broadband supercontinuum with a modulated polarization gating," *Opt. Express* **16**, 9795-9803 (2008).
14. W. Hong, P. Lu, Q. Li, and Q. Zhang, "Broadband water window supercontinuum generation with a tailored mid-IR pulse in neutral media," *Opt. Lett.* **34**, 2102-2104 (2009).
15. P. Lan, P. Lu, Q. Li, W. Hong, and Q. Zhang, "Macroscopic effects for quantum control of broadband isolated attosecond pulse generation with a two-color field," *Phys. Rev. A* **79**, 043413 (2009).
16. W. Cao, P. Lu, P. Lan, X. Wang, and Y. Li, "Control of the launch of attosecond pulses," *Phys. Rev. A* **75**, 063423 (2007).
17. J. E. Muffett, C. G. Wahlström, and M. H. R. Hutchinson, "Numerical modelling of the spatial profiles of high-order harmonics," *J. Phys. B* **27**, 5693-5706 (1994).
18. M. Lewenstein, P. Salières, and A. L'Huillier, "Phase of the atomic polarization in high-order harmonic generation," *Phys. Rev. A* **52**, 4747 (1995).
19. P. Salières, T. Ditmire, K. S. Budil, M. D. Perry, and A. L'Huillier, "Spatial profiles of high-order harmonics generated by a femtosecond Cr:LiSAF laser," *J. Phys. B* **27**, L217-L222 (1994).
20. P. Salières, A. L'Huillier, and M. Lewenstein, "Coherence Control of High-order Harmonics," *Phys. Rev. Lett.* **74**, 3776 (1995).
21. V. Tosa, H. T. Kim, I. J. Kim, and C. H. Nam, "High-order harmonic generation by chirped and self-guided femtosecond laser pulses. I. Spatial and spectral analysis," *Phys. Rev. A* **71**, 063807 (2005).
22. Y. Tamaki, J. Itatani, M. Obara, and K. Midorikawa, "Optimization of conversion efficiency and spatial quality of high-order harmonic generation," *Phys. Rev. A* **62**, 063802 (2000).
23. M. Lewenstein, Ph. Balcou, M. Yu. Ivanov, A. L'Huillier, and P. B. Corkum, "Theory of high-harmonic generation by low-frequency laser fields," *Phys. Rev. A* **49**, 2117 (1994).
24. M. V. Ammosov, N. B. Delone, and V. P. Krainov, "Tunnel ionization of complex atoms and of atomic ions in an alternating electromagnetic field," *Sov. Phys. JETP* **64**, 1191 (1986).
25. E. Priori, G. Cerullo, M. Nisoli, S. Stagira, S. D. Silvestri, P. Villoresi, L. Poletto, P. Ceccherini, C. Altucci, R. Bruzzese, and C. de Lisio, "Nonadiabatic three-dimensional model of high-order harmonic generation in the few-optical-cycle regime," *Phys. Rev. A* **61**, 063801 (2000).
26. W. Cao, P. Lu, P. Lan, X. Wang, and G. Yang "Single-attosecond pulse generation with an intense multicycle driving pulse," *Phys. Rev. A* **74**, 063821 (2006).
27. M. B. Gaarde, J. L. Tate, and K. J. Schafer, "Macroscopic aspects of attosecond pulse generation," *J. Phys. B* **41**, 132001 (2008).
28. A. L'Huillier, P. Balcou, S. Candel, k. J. Schafer, and K. C. Kulander, "Calculations of high-order harmonic-generation processes in xenon at 1064 nm," *Phys. Rev. A* **46**, 2778 (1992).

1. Introduction

The generation of extreme ultraviolet attosecond pulses has open new fields of time-resolved studies with high precision. An isolated attosecond pulse is an important tool for detecting and controlling the electronic dynamics inside atoms, such as innershell electronic relaxation and ionization by optical tunnelling [1]. Nowadays, various schemes including stimulated Raman scattering [2], Thomson Scattering [3,4], high-order harmonic generation (HHG) [5,6] and so on, have been explored for the generation of attosecond pulse. Currently, the production of isolated attosecond pulses is mainly based on HHG [7-9]. The first successful method to produce isolated attosecond pulses is using a few-cycle laser pulse, and 10-eV supercontinuum is obtained, which only supports an attosecond pulse of 250as [1]. The pulse duration of the attosecond pulse is greater than the natural time scale of the electronic process inside atoms (150as), and then its applications are significantly limited. Many efforts have been paid to broaden the bandwidth of the supercontinuum and shorten the pulse duration. In a recent work, Goulielmakis *et al.* has employed an extremely short laser pulse of 3.3fs to produce a 40-eV supercontinuum [10]. However, the duration of the driving pulse can hardly be further compressed, and the applications of the attosecond pulse are limited due to the low output energy. It is still challenging to further broaden and enhance supercontinuum.

The process of HHG is well understood with the three-step model [11], which shows that the ionization, acceleration and recombination of the electrons determine the time-frequency characteristics of the harmonic generation. The three steps of HHG process can be controlled

to generate a broadband supercontinuum. It has been proposed that the attosecond pulse bandwidth can be effectively broadened in the polarization-gate scheme [12,13], which can control the recombination of the electrons in the laser field. The two-color field scheme is a promising way to produce the broadband supercontinuum by controlling the electron acceleration (acceleration gating, AG) and ionization (ionization gating, IG) processes [14,15]. Lan et al [15] found that the broadband supercontinuum in the AG scheme can be generated in the cutoff, while the IG scheme produces the supercontinuous high harmonics in the plateau and the harmonic and attosecond pulse yields are higher.

Recent studies mainly focus on the spectral and temporal characteristics of HHG for the goal of the generation of high-efficiency attosecond pulse [10-16], but its spatial characteristics have seldom been investigated. The studies on the spatial characteristics of HHG in the monochromatic field have been reported in the previous works [17-22]. Salières [19] *et al.* found that the spatial profile of the harmonic in the cutoff region is almost Gaussian in experiment using one-color laser pulse. Moreover, the same group demonstrated that the spatial properties can be controlled and optimized by moving the laser focus position relative to the nonlinear medium [20]. Recently, Tosa *et al.* [21] pointed out that the chirp of laser field can change the spatial distribution of high-order harmonic generation. Temporal and spatial modifications of the laser pulse can influence the harmonic field both in spectral and spatial characteristics [21]. In the two-color scheme, the laser beam is modified by temporal distribution of the controlling field, and then broadband supercontinuum can be generated effectively. The spatial quality optimization of the supercontinuum is the important issue in many applications, which has been seldom investigated. In this paper, we investigate that spatial characteristics of xuv supercontinuum generation in the $\omega + 2\omega$ laser field. By optimizing the synthesized two-color field, the spatial profile of the xuv supercontinuum varies from annular-like to Gaussian-like, which implies that the spatial quality can be controlled and improved effectively. Moreover, our calculation shows that the spatial quality of the supercontinuum is stable when the intensity of the controlling field varies in the acceptable fluctuation.

2. Theoretical model

The theoretical description of HHG takes into account both the single-atom response (SAR) to the laser pulse and the collective response of macroscopic gas to the laser and high harmonic fields. In our simulation, SAR is calculated with Lewenstein model [23] and the nonlinear dipole momentum is [in atomic units (a.u.)]

$$d_{nl}(t) = i \int_{-\infty}^t dt' \left[\frac{\pi}{\varepsilon + i(t-t')/2} \right]^{3/2} \times d^* [p_{st}(t',t) - A(t)] d [p_{st}(t',t) - A(t')] \times \exp [-iS_{st}(t',t)] E(t')g(t') + c.c.. \quad (1)$$

In the Eq. $E(t)$ is the electric field, $A(t)$ is the vector potential. ε is a positive regularization constant. p_{st} and S_{st} are the stationary momentum and quasiclassical action, which are given by

$$p_{st}(t',t) = \frac{1}{t-t'} \int_{t'}^t A(t'') dt'', \quad (2)$$

$$S_{st}(t',t) = (t-t')I_p - \frac{1}{2} p_{st}^2(t',t)(t-t') + \frac{1}{2} \int_{t'}^t A^2(t'') dt'', \quad (3)$$

where I_p is the ionization energy of the helium. $d(p)$ is the dipole matrix element for transitions from the ground state to the continuum state. For hydrogenlike atoms, it can be written as

$$d(p) = i \frac{2^{7/2}}{\pi} (2I_p)^{5/4} \frac{p}{(p^2 + 2I_p)^3}. \quad (4)$$

$g(t)$ in the Eq. (1) represents the ground state amplitude:

$$g(t') = E_f(t') \exp \left[- \int_{-\infty}^{t'} \omega(t') dt' \right]. \quad (5)$$

$\omega(t')$ is the ionization rate, which is calculated by Ammosov-Delone-Krainov (ADK) tunnelling model [24]:

$$\omega(t) = w_e |C_{n^*}|^2 \left(\frac{4w_e}{\omega_t} \right)^{2n^*-1} \exp \left(- \frac{4w_e}{3\omega_t} \right), \quad (6)$$

$$d(p) = i \frac{2^{7/2}}{\pi} (2I_p)^{5/4} \frac{p}{(p^2 + 2I_p)^3}. \quad (7)$$

$$w_e = \frac{I_p}{\hbar}, \omega_t = \frac{e|E_l(t)|}{\sqrt{2m_e I_p}}, n^* = Z \left(\frac{I_{ph}}{I_p} \right)^{1/2}, |C_{n^*}|^2 = \frac{2^{2n^*}}{n^* \Gamma(n^* + 1) \Gamma(n^*)}, \quad (8)$$

where Z is the net resulting charge of the atom, I_{ph} is the ionization potential of the hydrogen atom, and e and m_e are electron charge and mass respectively.

To simulate the collective response of macroscopic gas, we solve the light propagation for the laser and high harmonic fields in cylindrical coordinate separately [25],

$$\nabla^2 E_l(r, z, t) - \frac{1}{c^2} \frac{\partial^2 E_l(r, z, t)}{\partial t^2} = \frac{\omega_p(r, z, t)^2}{c^2} E_l(r, z, t), \quad (9)$$

$$\nabla^2 E_h(r, z, t) - \frac{1}{c^2} \frac{\partial^2 E_h(r, z, t)}{\partial t^2} = \frac{\omega_p(r, z, t)^2}{c^2} E_h(r, z, t) + \mu_0 \frac{\partial^2 P_{nl}(r, z, t)}{\partial t^2}, \quad (10)$$

where E_l and E_h are the laser field and high harmonics, respectively. ω_p is the plasma frequency and is given by

$$\omega_p = e \sqrt{\frac{n_e(r, z, t)}{m \epsilon_0}} \quad (11)$$

The nonlinear polarization of gas is $P_{nl} = n_0 d_{nl}$. n_0 and n_e are the densities of neutral atoms and free electrons. The electron density can be expressed as

$$n_e(t) = n_0 [1 - \exp(- \int_{-\infty}^t \omega(t') dt')], \quad (12)$$

3. Result and discussion

In this work, the two-color field is synthesized by a 5-fs linearly polarized driving pulse with a wavelength of 800 nm and a 5-fs linearly polarized control pulse with a wavelength of 400 nm. The peak intensities of the driving and control pulses are $6 \times 10^{14} \text{ W/cm}^2$ and $2.4 \times 10^{13} \text{ W/cm}^2$, respectively. The electric field of the synthesized laser pulse is expressed by

$$E(t) = E_0 f(t) \cos[\omega_0(t)] + E_1 f(t) \cos[2\omega_0(t) + \phi_0], \quad (13)$$

E_0 and E_1 are the amplitudes of the driving and controlling field. $f(t)$ and ω_0 are the envelope and the frequency. A Gaussian envelope shape is adopted and ϕ_0 is set as 0.

We first compare the spectral characteristics of HHG in the two-color field with those in one-color field using Lewenstein model [23, 26]. In the two-color field, by mixing a control laser pulse to the fundamental pulse, the synthesized field can be shaped, which results in the different spectral characteristics of HHG from those in one-color case. The electric field of the two-color field (red solid curve) synthesized by the fundamental (green solid curve) and controlling (the blue dashed curve) fields is shown in Fig. 1(a). The ionization probability in the two-color field is represented by the red dashed line. As shown in Fig. 1(a), the controlling field is in the same direction with the fundamental field at the peak P, where the intensity of the synthesized field is enhanced. Thus, the ionization of the electron is enhanced at P. Further, HHG is also confined within this half-cycle optical cycle. This scheme is named the ionization gate (IG). The harmonic spectrum in the two-color field is presented by the red solid curve in Fig. 1(b). For comparison, the spectrum of HHG in the fundamental field alone is also presented (the green solid curve). As shown in Fig. 1(b), the spectral structure in one-color field is irregular for the harmonics in the plateau and becomes continuous for the harmonics in the cutoff. However, the overall spectrum in the two-color field becomes smooth and regularly modulated for the harmonics through the plateau to cutoff. What's more, the efficiency of the HHG in the plateau is enhanced by about one order. Our calculation shows that the broadband supercontinuum in the two-color field is generated in the plateau and the yield of the harmonics is higher than that in the one-color field.

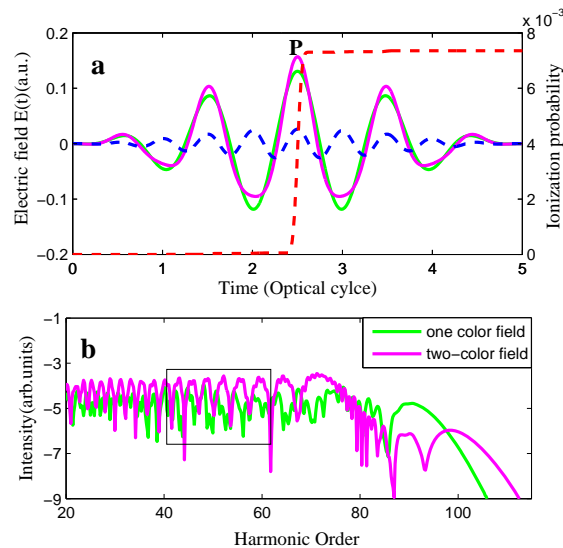


Fig. 1. (a), The electric field of the two-color field (red solid curve) synthesized by the fundamental (green solid curve) and controlling (the blue dashed curve) fields, the ionization probability in the two-color field is presented by the red dashed line. (b), The harmonic spectrum in the two-color field (the red solid curve) and in the fundamental field alone (the green solid curve)

Next, we investigate the spatial characteristics of the efficient broadband supercontinuum described above. For convenience, the harmonics from 40th-60th in the plateau are taken as our

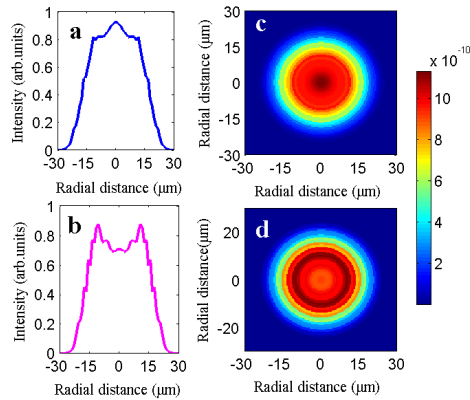


Fig. 2. The near-field spatial profiles of 40th-60th harmonics at the exit of the medium in the one-color field (a) and the two-color field (b), and the corresponding spatial images of the harmonics are also presented in (c) and (d).

object of study. In the nonadiabatic three-dimensional propagation simulations [25], we utilize a 0.45-mm long gas target with a density of $1.37 \times 10^{18}/\text{cm}^3$, which corresponds to a gas pressure of 40 Torr at room temperature. The focuses of the fundamental field and controlling field are put at the same position and the beam waists are both $25\mu\text{m}$. The entrance of the gas jet is placed 2 mm after the focuses of the laser field. Other parameters are the same as in Fig. 1. The near-field spatial profiles of 40th-60th harmonics at the exit of the medium in the one-color and the two-color fields are shown in Fig. 2, and the corresponding spatial images of the harmonics are also represented in Figs. 2(c) and (d). In the one-color field in Figs. 2(a) and (c), the near-field spatial profile of 40th-60th harmonics in the fundamental field alone is Gaussian-like. It is believed that the spatial quality of HHG with a Gaussian profile is better than that with an annular-like profile, and then the high-order harmonics in the one-color field has a good spatial quality. As we known, the spatial distribution of the laser field and phase matching of HHG in macroscopic medium play an important role in the spatial profile of HHG. When the laser focus is put before the gas target, short trajectory is preferably selected in the propagation and better phase matching of the short trajectory contribution to harmonics in the plateau is obtained off-axis [27]. However, the incident one-color field is Gaussian in space, which results in Gaussian distribution of high-order harmonic generation. Figure 2(b) shows the near-field spatial profile of HHG in the two-color field. Compared with those in one-color case, the near-field spatial profile of HHG in the two-color case is an annular-like distribution, which implies that the spatial quality of the supercontinuum in the two-color case is poor.

The poor spatial quality of the supercontinuum in the two-color field limits its potential applications. We propose an efficient method to control and improve the spatial quality of the broadband supercontinuum by optimizing the synthesized field. Figure 3 shows the near-field spatial images and profiles of HHG in the two-color field with different focus positions and beam waists of the controlling field. In Figs. 3(a) and (e), the parameters are the same as those in Fig. 2(b), and the spatial profile of the HHG is annular-like. The spatial quality is not improved when the beam waist and focus position of the controlling field are $25\mu\text{m}$ and 0mm (seen in Figs. 3(b) and (f)). However, when the beam waist of the controlling field is further decreased to $20\mu\text{m}$ and the corresponding focus position is 0mm (seen in Figs. 3(c) and (g)), the spatial profile of the HHG becomes a similar rectangle. When the beam waist of the controlling field

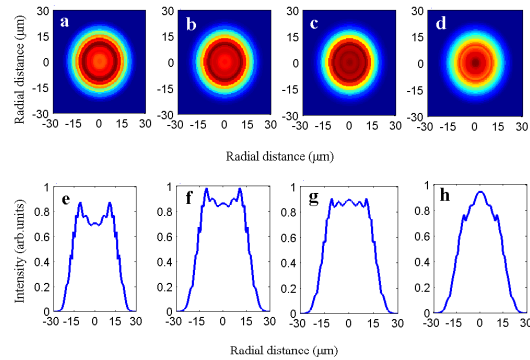


Fig. 3. The near-field spatial images and profiles of HHG in the two-color field with different beam waists and focus positions of the controlling field. The beam waist and focus position are set as $25\mu\text{m}$ and 2mm (a and e), $25\mu\text{m}$ and 0mm (b and f), $20\mu\text{m}$ and 0mm (c and g), $15\mu\text{m}$ and 0mm (d and h), respectively. The other parameters are same in Fig. 2(b).

is reduced to $15\mu\text{m}$ and the focus position is 0mm (seen in Figs. 3(d) and (h)), the harmonic profile becomes nearly Gaussian, which implies that the spatial quality of the supercontinuum has been optimized. Figure 3 shows that the spatial quality of the broadband supercontinuum in the two-color field can be effectively controlled and optimized.

Figure 4(b) shows the far-field spatial profiles of the supercontinuum[28]. For comparison, the near-field spatial profiles in Figs. 3(e) and (h) are represented by the red dashed and blue curve in Fig. 4(a), respectively. The near-field spatial profile represented by the red dashed in Fig. 4(a) is annular-like, and the corresponding far-field spatial quality in Fig. 4(b) is a little improved, which is rectangle-like. When the near-field spatial profile represented by the blue curve is Gaussian-like, the far-field spatial profile is also the Gaussian-like and the divergence angle is smaller than that of the similar rectangle profile.

The spatial distribution of the two-color field influences critically the spatial profile of the harmonic generation. Figure 4 shows the integral of the two-color field at the ionization times of the trajectories corresponding to the 40th-60th harmonics in the plateau. The parameters in Figs. 5(a) and (b) are the same as those in Figs. 3(a) and (d), respectively. For the single-atom response, when the intensity of the laser pulse is much lower than the saturation intensity of the model atom, the harmonic efficiency is mainly determined by the ionization rate. As shown in Fig. 3(a), the laser field off the propagation axes is more intense than that on the axes, which results in higher ionization rate off the propagation axes. Thus, brighter harmonic field can be generated off the axes. However, when the beam waist of the controlling field is $15\mu\text{m}$ and the focus position is 0mm (seen in Fig. 5(b)), the laser field on the propagation axes is more intense than that off the axes, thus the harmonics on the axes (seen in Fig. 3(d)) is brighter than that off the axes. It is shown that the integral maps of the two-color field at the ionization times of the trajectories corresponding to the 40th-60th harmonics are consistent with the spatial distribution of HHG.

Last, we investigate the influence of the focus position and intensity of the controlling field on the spatial characteristics of the broadband supercontinuum. In Fig. 6(a), the focus position of the controlling field is changed and other parameters are the same as those in Fig. 3(d). When the focus position of the controlling field is 2mm , the spatial profile of HHG is annular-like,

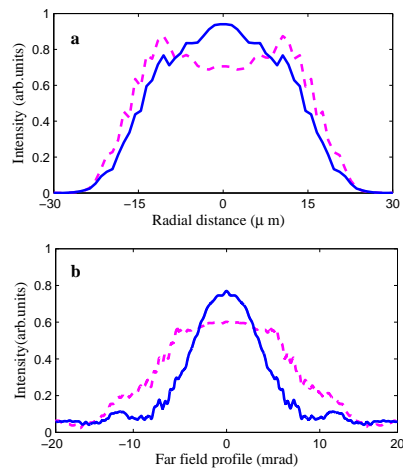


Fig. 4. The near-field (a) and the corresponding far-field (b) profiles of HHG: The beam waist and focus position of the controlling field are set as $25\mu\text{m}$ and 2mm (the red dashed), $15\mu\text{m}$ and 0mm (the red curve).

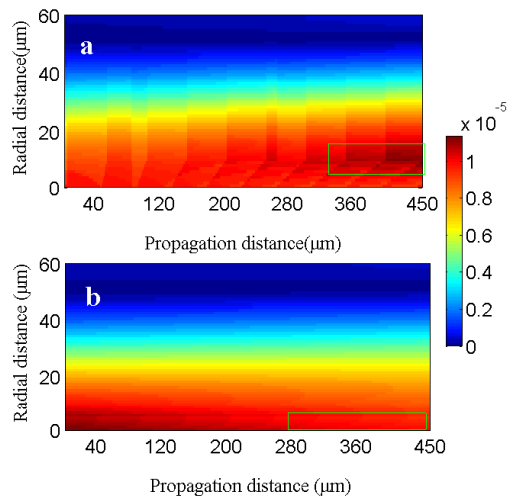


Fig. 5. The integral of the laser field at the ionization times of the trajectories corresponding to the 40th-60th harmonics in the plateau. The parameters in Figs. 4(a) and (b) are the same as those in Figs. 3(a) and (d), respectively.

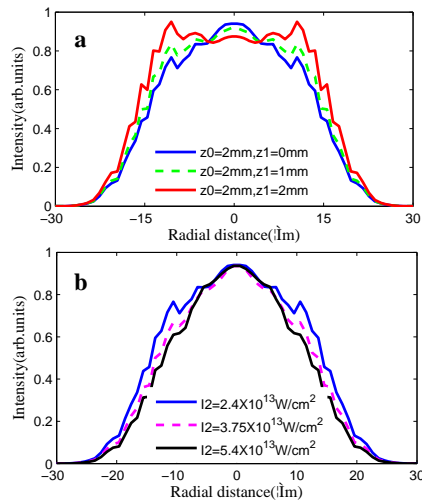


Fig. 6. (a) the spatial profiles of HHG in the two-color field with different focus positions z_1 of the controlling field, the other parameters are the same as these in Fig. 3(d). (b) the spatial profiles of HHG in the two-color field with different relative intensities I_2 of the controlling field.

which implies that the intensity of HHG off the axes is more intense than that on the axes. As the focus position is set as 1mm or 0mm , the spatial profile of HHG becomes Gaussian-like. Figure 6(b) shows that the spatial profiles of HHG in the two-color field with different intensities of the controlling field. Other parameters are the same as those in Fig. 3(d). As shown in Fig. 6(b), the spatial profiles of HHG for the different intensities I_2 of the controlling field are all the Gaussian-like shape. When the intensity of the controlling is increased from $2.4 \times 10^{13} \text{W/cm}^2$ to $5.4 \times 10^{13} \text{W/cm}^2$, i.e. the relative intensity varies from 0.04 to 0.09, the divergence angle of HHG becomes smaller. From Fig. 6, it is shown that the spatial profile of the supercontinuum is stability to the intensity variation of the controlling field and sensitivity to the focus position.

4. Conclusion

In conclusion, we have investigated the spectral and spatial characteristics of xuv supercontinuum generation in the $\omega + 2\omega$ laser field. It is shown that HHG can be confined within half optical cycle in the two-color field and then high-efficiency supercontinuum is generated in the plateau, while the spatial profile of the supercontinuum is an annular-like distribution, which limits its application. By optimizing the two-color field, the spatial profile of the xuv supercontinuum varies from annular-like to Gaussian-like, which shows that the spatial quality of the supercontinuum in the two-color field can be controlled and optimized effectively. Moreover, when the relative intensity the controlling field varies from 0.04 to 0.09, the spatial profile of the supercontinuum shows stability.

Acknowledgment

This work was supported by the National Natural Science Foundation of China under Grants No.60925021,10904045,10734080, and the National Key Basic Research Special Foundation under Grant No.2011CB808103.